Synthesis and crystal structure of di-*μ*-methoxo-bis(oxido{*N′*-[3-(oxidoimino)butan-2-ylidene]-benzohydrazonato-*κ*³*O,N,O′*}vanadium(V))

Nirupama Saladi* and Ankit Kumar Srivastava

School of Chemistry, University of Hyderabad, Hyderabad 500 046, India. *Correspondence e-mail: 19chph09@uohyd.ac.in

The structure of the dimeric oxomethoxovanadium(V) complex, $[V_2(CH_3O)_2(C_{11}H_{11}N_3O_3)_2]$ or $[VO(\mu\text{-OMe})(L)]_2$ (**1**), with N'-[3-(hydroxy-imino)-butan-2-ylidene]benzohydrazide (H_2L, where 2 Hs represent the dissociable oxime and amide protons) is reported. The oximate functionality can coordinate through either the O or the N atom. In the present complex, it is coordinated through the O atom. Here, methoxo groups bridge the two V^V centers with a V···V separation of 3.3275 (10) Å. Within the centrosymmetric edge-shared dioctahedral structure, each metal center is in a distorted octahedral NO_5 environment, assembled by the O,N,O-donor L^{2-} ligand, bridging OMe^- groups and the oxo group. The complex is diamagnetic in nature and brown in color. Solution electrical conductivity measurements confirmed its electrically non-conducting behavior.

1. Chemical context

Interest in the coordination complexes of vanadium is primarily due to their variety of roles in biological processes such as nitrogen fixation, haloperoxidation, phosphorylation, insulin mimicking, anti-microbial and anti-fungal activities, and for their possible use as efficient catalysts in various organic reactions (Noblía *et al.*, 2004; Plass *et al.*, 2007; Zabin & Abdelbaset, 2016; Tsave *et al.*, 2016; Tanabe & Nishibayashi, 2019; Assey & Mgohamwende, 2020). Oxovanadium(V) (VO^{3+}) and dioxovanadium(V) (VO_2^+) catalyzed reactions include C—C bond formation, hydrogenation, dehydrogenation, sulfide oxidation, C—C/C—O bond cleavage, alcohol/aldehyde/ketone oxidation, deoxydehydration (Langeslay *et al.*, 2019). Oxovanadium(IV/V) materials have also found several industrial applications such as gas sensors, electrochemical and optical switching devices, and reversible cathode materials for Li batteries (Guerrero-Pérez, 2017).

H_2L

$[VO(\mu\text{-OMe})(L)]_2$

Our research group has previously reported some penta-valent vanadium complexes with aroylhydrazine-based Schiff bases (Srivastava *et al.*, 2020). Herein we report a dinuclear

Table 1
Selected geometric parameters (Å, °).

V1—O4	1.5795 (16)	V1—O2	1.9469 (14)
V1—O1	1.8200 (16)	V1—N2	2.1013 (16)
V1—O3	1.8351 (14)	V1—O3^i	2.3240 (14)
O4—V1—O1	100.13 (9)	O2—V1—N2	74.61 (6)
O4—V1—O3	103.30 (7)	O4—V1—O3^i	177.40 (7)
O1—V1—O3	107.22 (7)	O1—V1—O3^i	79.72 (7)
O4—V1—O2	100.48 (8)	O3—V1—O3^i	74.33 (6)
O1—V1—O2	149.15 (7)	O2—V1—O3^i	80.69 (6)
O3—V1—O2	90.01 (6)	N2—V1—O3^i	87.30 (5)
O4—V1—N2	95.24 (7)	C12—O3—V1^i	124.22 (14)
O1—V1—N2	80.87 (6)	V1—O3—V1^i	105.67 (6)
O3—V1—N2	157.85 (6)		

Symmetry code: (i) $-x, -y + 1, -z$.

centrosymmetric complex $[VO(\mu\text{-OMe})(L)]_2$, where we have used an ambidentate oxime containing N'-[3-(hydroxyimino)butan-2-ylidene]benzohydrazide (H_2L).

2. Structural commentary

The dimeric complex $[VO(\mu\text{-OMe})(L)]_2$ (**1**) crystallizes in the triclinic $P\bar{1}$ space group. Here the asymmetric unit contains half of the formula unit and the two halves of the dimeric molecule are related by an inversion center. A displacement ellipsoid plot of **1** is illustrated in Fig. 1. The meridionally spanning L^{2-} coordinates to the metal center *via* the oximate-O, the imine-N and the amidate-O atoms (O1, N2 and O2, respectively) and forms fused five- and six-membered chelate rings. The methoxo-O atom (O3) completes an NO_3 square plane (r.m.s. deviation = 0.02 Å) and the oxo group (O4)
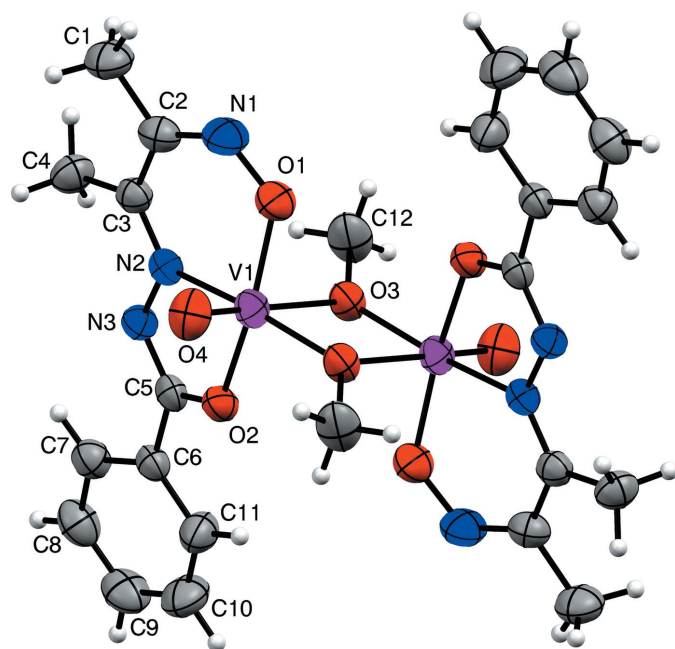

Figure 1
The molecular structure of $[VO(\mu\text{-OMe})(L)]_2$ (**1**). The non-hydrogen atoms are displayed as 30% probability ellipsoids. Unlabeled non-hydrogen atoms are related to the labeled non-hydrogen atoms by an inversion center (symmetry operator: $-x, -y + 1, -z$).

Table 2
Hydrogen-bond geometry (Å, °).

D—H$\cdots A$	D—H	H$\cdots A$	$D \cdots A$	D—H$\cdots A$
C1—H1$A \cdots$O4^{ii}	0.96	2.98	3.583 (3)	122
C1—H1$A \cdots$N1^{iii}	0.96	3.02	3.508 (3)	113
C4—H4$A \cdots$N3^{iv}	0.96	2.81	3.663 (3)	149
C12—H12$B \cdots$O2^{v}	0.96	2.96	3.531 (3)	119
C12—H12$C \cdots$O4^{v}	0.96	2.81	3.629 (3)	144

Symmetry codes: (ii) $-x, -y + 1, -z + 1$; (iii) $-x + 1, -y + 1, -z + 1$; (iv) $-x, -y, -z$; (v) $-x - 1, -y + 1, -z$.

occupies the apical position to complete a square-pyramidal NO_4 coordination environment around the metal center. As generally observed in a square-pyramidal geometry, here the vanadium atom is also shifted towards the apical oxo group by 0.34 Å. The dimeric structure is formed by two such inversion-symmetry-related square-pyramidal units, in which the methoxo-O atoms act as equatorial–axial bridging atoms. As a result, a divanadium(V) core, $[OV(\mu\text{-OMe})_2VO]^{4+}$, is formed at the center of **1** and each metal center in it resides in a distorted octahedral NO_5 coordination sphere. Overall, two O,N,O-donor L^{2-}, two methoxo-O atoms, and the two oxo-O atoms constitute an edge-shared dioctahedral geometry $[O_3NVO_2VNO_3]$ (Fig. 1). The central $V_2(\mu\text{-OMe})_2$ moiety has a pair of short [1.8351 (14) Å] and a pair of long [2.3240 (14) Å] V—O bonds (Table 1). The longer pair of bonds is *trans* to the corresponding oxo groups. The V$\cdots$V distance is 3.3275 (10) Å. In general, the V=O, V—N, and V—O bond lengths in **1** are comparable with the corresponding bond lengths in other pentavalent vanadium complexes with analogous ligands (Dash *et al.*, 2012; Sutradhar *et al.*, 2013; Srivastava *et al.*, 2018; Srivastava *et al.*, 2020).

3. Supramolecular features

We have investigated the self-assembly pattern of complex **1** *via* intermolecular hydrogen-bonding interactions having an H$\cdots A$ distance of up to 3 Å. Only non-classical C—H$\cdots A$ (A = O and N) interactions have been found (Table 2). These are: one bifurcated C—H$\cdots$O/N, two C—H$\cdots$O and one C—H$\cdots$N interactions involving the methyl C—H (C1—H1A and C4—H4A) and methoxo C—H groups (C12—H12B and
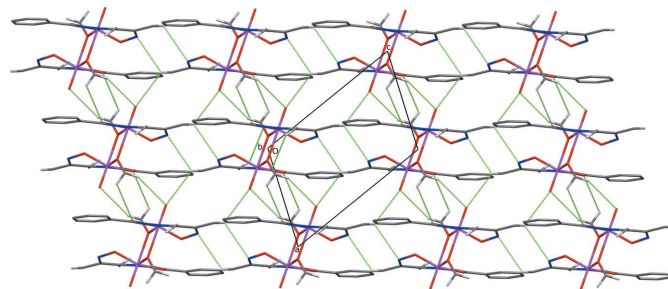

Figure 2
Three-dimensional network of **1** viewed down the *b*-axis. Green dashed lines indicate non-classical hydrogen bonds listed in Table 2. Hydrogen atoms not involved in these interactions are omitted for clarity.

Table 3
Experimental details.

Crystal data	
Chemical formula	$[V_2(CH_3O)_2(C_{11}H_{11}N_3O_3)_2]$
M_r	630.40
Crystal system, space group	Triclinic, $P\bar{1}$
Temperature (K)	298
a, b, c (Å)	7.3050 (16), 9.825 (2), 11.121 (3)
α, β, γ (°)	105.586 (8), 107.226 (8), 101.610 (9)
V (Å³)	699.3 (3)
Z	1
Radiation type	Mo $K\alpha$
μ (mm^{-1})	0.73
Crystal size (mm)	$0.23 \times 0.22 \times 0.21$
Data collection	
Diffractometer	Bruker APEXII CCD
Absorption correction	Multi-scan (SADABS; Krause et al., 2015)
T_{min}, T_{max}	0.851, 0.863
No. of measured, independent and observed [$I > 2\sigma(I)$] reflections	26928, 2849, 2495
R_{int}	0.046
$(\sin \theta/\lambda)_{max}$ (Å^{-1})	0.626
Refinement	
$R[F^2 > 2\sigma(F^2)]$, $wR(F^2)$, S	0.032, 0.085, 1.05
No. of reflections	2849
No. of parameters	184
H-atom treatment	H-atom parameters constrained
$\Delta\rho_{max}, \Delta\rho_{min}$ (e Å^{-3})	0.24, −0.29

Computer programs: APEX2 and SAINT (Bruker, 2014), SHELXS97 (Sheldrick 2008), SHELXL2014/7 (Sheldrick 2015), Mercury (Macrae et al., 2020), and WinGX publication routines (Farrugia, 2012).

C12—H12C) as donors, and iminolate-O (O2), oxo-O (O4), oximate-N (N1), and imine-N (N3) atoms as acceptors. The C—H⋯O (C12—H12B⋯O2 and C12—H12C⋯O4) interactions link the complex molecules and form linear chains parallel to each other. The bifurcated C—H⋯O/N (C1—H1A⋯O4/N1) hydrogen bonds connect the parallel linear chains and a di-periodic layered structure is formed. The C—H⋯N (C4—H4A⋯N3) interactions provide the links between the layers, assembling a three-dimensional network structure (Fig. 2).

4. Database survey

Five more structures of analogous dinuclear dimethoxo bridged oxovanadium(V) complexes are reported in the literature and deposited in the Cambridge Structure Database (CSD v5.43; Groom et al., 2016). These are [VO(μ-OMe)(L^1)]$_2$ (CSD refcode XIVJUH) with H$_2$L^1 = benzoylhydrazone of 2-hydroxy-5-methoxybenzaldehyde (Sangeetha et al., 2000), [VO(μ-OMe)(L^2)]$_2$ (CSD: GAVROL) with H$_2$L^2 = diacetyl monoxime (4-methoxybenzoyl)hydrazone (Deng et al., 2005), [VO(μ-OMe)(L^3)]$_2$ (CSD: KUBSUW) with H$_2$L^3 = benzoic acid (1-methyl-3-oxo-butylidene)hydrazide, [VO(μ-OMe)(L^4)]$_2$ (CSD: KUBTAD) with H$_2$L^4 = 4-Cl-benzoic acid (1-methyl-3-oxo-butylidene)hydrazide (Sarkar & Pal, 2009), and [VO(μ-OMe)(HL^5)]$_2$ (CSD: FUDTUW) with H$_3$L^5 = diacetylmonoxime salicyloylhydrazone (Srivastava et al., 2020).

5. Synthesis and crystallization

The Schiff base (H$_2$L) was prepared in ∼72% yield by a condensation reaction with equimolar amounts of diacetylmonoxime and benzohydrazide in methanol, following a reported procedure (Naskar et al., 2007).

A methanol solution (10 ml) of [VO(acac)$_2$] (80 mg, 0.3 mmol) was added to a methanol solution (10 ml) of H$_2$L (65 mg, 0.3 mmol) and the mixture was stirred under aerobic conditions for 6 h at room temperature. The resulting brown solution was kept for slow evaporation at room temperature in air. The dark-brown crystalline material was obtained in about a week. It was filtered, washed with cold methanol, and dried in air. A single crystal suitable for X-ray structure determination was selected from the crystals thus obtained. Yield: 47 mg (50%). HRMS in acetonitrile m/z found (calculated) for ([M + Li]$^+$): 637.3059 (637.1008).

6. Refinement

Crystal data, data collection and structure refinement details are summarized in Table 3. All non-hydrogen atoms were refined anisotropically. A riding model was used to include all hydrogen atoms at idealized positions with C—H distances of 0.93 Å (C$_{ar}$—H) and 0.96 Å (C$_{Me}$—H) and U_{iso} = 1.2 or 1.5 U_{eq} of the attached carbon atom.

References

Assey, G. E. & Mgohamwende, R. (2020). Pharm. & Pharmacol. Int. J. 8, 136–146.
Bruker (2014). APEX2 and SAINT. Bruker AXS Inc., Madison, Wisconsin, USA.
Dash, S. P., Pasayat, S., Saswati, Dash, H. R., Das, S., Butcher, R. J. & Dinda, R. (2012). Polyhedron, 31, 524–529.
Deng, Z.-P., Gao, S., Huo, L.-H. & Zhao, H. (2005). Acta Cryst. E61, m2214–m2216.
Farrugia, L. J. (2012). J. Appl. Cryst. 45, 849–854.
Groom, C. R., Bruno, I. J., Lightfoot, M. P. & Ward, S. C. (2016). Acta Cryst. B72, 171–179.
Guerrero-Pérez, M. O. (2017). Catal. Today, 285, 226–233.
Krause, L., Herbst-Irmer, R., Sheldrick, G. M. & Stalke, D. (2015). J. Appl. Cryst. 48, 3–10.
Langeslay, R. R., Kaphan, D. M., Marshall, C. L., Stair, P. C., Sattelberger, A. P. & Delferro, M. (2019). Chem. Rev. 119, 2128–2191.
Macrae, C. F., Sovago, I., Cottrell, S. J., Galek, P. T. A., McCabe, P., Pidcock, E., Platings, M., Shields, G. P., Stevens, J. S., Towler, M. & Wood, P. A. (2020). J. Appl. Cryst. 53, 226–235.

Naskar, S., Mishra, D., Butcher, R. J. & Chattopadhyay, S. K. (2007). *Polyhedron*, **26**, 3703–3714.

Noblía, P., Baran, E. J., Otero, L., Draper, P., Cerecetto, H., González, M., Piro, O. E., Castellano, E. E., Inohara, T., Adachi, Y., Sakurai, H. & Gambino, D. (2004). *Eur. J. Inorg. Chem.* pp. 322–328.

Plass, W., Bangesh, M., Nica, S. & Buchholz, A. (2007). *Model Studies of Vanadium-Dependent Haloperoxidation: Structural and Functional Lessons*, ACS Symposium Series, Vol. 974, pp. 163–177. Washington: American Chemical Society.

Sangeetha, N. R., Kavita, V., Wocadlo, S., Powell, A. K. & Pal, S. (2000). *J. Coord. Chem.* **51**, 55–66.

Sarkar, A. & Pal, S. (2009). *Inorg. Chim. Acta*, **362**, 3807–3812.

Sheldrick, G. M. (2008). *Acta Cryst.* A**64**, 112–122.

Sheldrick, G. M. (2015). *Acta Cryst.* C**71**, 3–8.

Srivastava, A. K., Ghosh, S., Jana, S. & Pal, S. (2018). *Inorg. Chim. Acta*, **483**, 329–336.

Srivastava, A. K., Ghosh, S. & Pal, S. (2020). *Inorg. Chim. Acta*, **502**, 119344.

Sutradhar, M., Roy Barman, T., Ghosh, S. & Drew, M. G. B. (2013). *J. Mol. Struct.* **1037**, 276–282.

Tanabe, Y. & Nishibayashi, Y. (2019). *Coord. Chem. Rev.* **381**, 135–150.

Tsave, O., Petanidis, S., Kioseoglou, E., Yavropoulou, M. P., Yovos, J. G., Anestakis, D. & Salifoglou, A. (2016). *Oxidative Med. Cell. Longev.* Article ID 4013639. https://doi.org/10.1155/2016/4013639

Zabin, S. A. & Abdelbaset, M. (2016). *Eur. J. Chem.* **7**, 322–328.

supporting information

Synthesis and crystal structure of di-*μ*-methoxo-bis(oxido{*N*′-[3-(oxidoimino)-butan-2-ylidene]benzohydrazonato-*κ³O,N,O*′}vanadium(V))

Nirupama Saladi and Ankit Kumar Srivastava

Computing details

Data collection: *APEX2* (Bruker, 2014); cell refinement: *SAINT* (Bruker, 2014); data reduction: *SAINT* (Bruker, 2014); program(s) used to solve structure: *SHELXS97* (Sheldrick 2008); program(s) used to refine structure: *SHELXL2014/7* (Sheldrick 2015); molecular graphics: *Mercury* (Macrae *et al.*, 2020); software used to prepare material for publication: *WinGX* publication routines (Farrugia, 2012).

Di-*μ*-methoxo-bis(oxido{*N*′-[3-(oxidoimino)butan-2-ylidene]benzohydrazonato-*κ³O,N,O*′}vanadium(V))

Crystal data

$[V_2(CH_3O)_2(C_{11}H_{11}N_3O_3)_2]$	$Z = 1$
$M_r = 630.40$	$F(000) = 324$
Triclinic, $P\bar{1}$	$D_x = 1.497$ Mg m^{-3}
$a = 7.3050$ (16) Å	Mo $K\alpha$ radiation, $\lambda = 0.71073$ Å
$b = 9.825$ (2) Å	Cell parameters from 9603 reflections
$c = 11.121$ (3) Å	$\theta = 3.0$–26.3°
$\alpha = 105.586$ (8)°	$\mu = 0.73$ mm^{-1}
$\beta = 107.226$ (8)°	$T = 298$ K
$\gamma = 101.610$ (9)°	Block, brown
$V = 699.3$ (3) Å^3	$0.23 \times 0.22 \times 0.21$ mm

Data collection

Bruker APEXII CCD diffractometer	2849 independent reflections
Radiation source: fine-focus sealed tube	2495 reflections with $I > 2\sigma(I)$
φ and ω scans	$R_{int} = 0.046$
Absorption correction: multi-scan (SADABS; Krause *et al.*, 2015)	$\theta_{max} = 26.4°$, $\theta_{min} = 2.5°$
$T_{min} = 0.851$, $T_{max} = 0.863$	$h = -9 \rightarrow 9$
26928 measured reflections	$k = -12 \rightarrow 12$
	$l = -13 \rightarrow 13$

Refinement

Refinement on F^2	Primary atom site location: structure-invariant direct methods
Least-squares matrix: full	Secondary atom site location: difference Fourier map
$R[F^2 > 2\sigma(F^2)] = 0.032$	
$wR(F^2) = 0.085$	
$S = 1.05$	Hydrogen site location: inferred from neighbouring sites
2849 reflections	H-atom parameters constrained
184 parameters	
0 restraints	

$w = 1/[\sigma^2(F_o^2) + (0.0355P)^2 + 0.3713P]$
  where $P = (F_o^2 + 2F_c^2)/3$
$(\Delta/\sigma)_{max} < 0.001$

$\Delta\rho_{max} = 0.24$ e Å^{-3}
$\Delta\rho_{min} = -0.29$ e Å^{-3}

Special details

Geometry. All esds (except the esd in the dihedral angle between two l.s. planes) are estimated using the full covariance matrix. The cell esds are taken into account individually in the estimation of esds in distances, angles and torsion angles; correlations between esds in cell parameters are only used when they are defined by crystal symmetry. An approximate (isotropic) treatment of cell esds is used for estimating esds involving l.s. planes.

Refinement. Refinement of F^2 against ALL reflections. The weighted R-factor wR and goodness of fit S are based on F^2, conventional R-factors R are based on F, with F set to zero for negative F^2. The threshold expression of $F^2 > 2\sigma(F^2)$ is used only for calculating R-factors(gt) etc. and is not relevant to the choice of reflections for refinement. R-factors based on F^2 are statistically about twice as large as those based on F, and R- factors based on ALL data will be even larger. The structure was solved by direct methods and refined on F^2 using full-matrix least-squares procedures.

Fractional atomic coordinates and isotropic or equivalent isotropic displacement parameters (Å²)

	x	*y*	*z*	U_{iso}*/U_{eq}
V1	−0.08607 (5)	0.44936 (3)	0.10918 (3)	0.03903 (12)
O1	0.1665 (2)	0.50789 (16)	0.23557 (15)	0.0541 (4)
O2	−0.29767 (19)	0.30059 (14)	−0.05246 (14)	0.0404 (3)
O3	−0.0981 (2)	0.58907 (14)	0.02824 (14)	0.0409 (3)
O4	−0.2093 (3)	0.48301 (18)	0.20281 (16)	0.0578 (4)
N1	0.2299 (3)	0.4859 (2)	0.35485 (19)	0.0553 (5)
N2	−0.0753 (2)	0.24395 (17)	0.12871 (16)	0.0359 (3)
N3	−0.2005 (2)	0.11897 (17)	0.01885 (15)	0.0369 (4)
C1	0.2508 (4)	0.3332 (3)	0.4857 (2)	0.0611 (6)
H1A	0.316716	0.428766	0.555551	0.092*
H1B	0.345953	0.279053	0.482381	0.092*
H1C	0.143345	0.279288	0.503827	0.092*
C2	0.1669 (3)	0.3528 (2)	0.3532 (2)	0.0454 (5)
C3	0.0332 (3)	0.2233 (2)	0.23344 (19)	0.0380 (4)
C4	0.0235 (3)	0.0707 (2)	0.2350 (2)	0.0484 (5)
H4A	0.011744	0.007875	0.148658	0.073*
H4B	−0.091311	0.031769	0.254590	0.073*
H4C	0.143812	0.074359	0.302670	0.073*
C5	−0.3129 (3)	0.1622 (2)	−0.06967 (19)	0.0355 (4)
C6	−0.4598 (3)	0.0488 (2)	−0.19731 (19)	0.0369 (4)
C7	−0.5068 (3)	−0.1011 (2)	−0.2135 (2)	0.0457 (5)
H7	−0.452941	−0.130314	−0.141287	0.055*
C8	−0.6331 (3)	−0.2060 (2)	−0.3364 (2)	0.0551 (6)
H8	−0.662785	−0.306194	−0.347149	0.066*
C9	−0.7154 (4)	−0.1640 (3)	−0.4428 (2)	0.0618 (6)
H9	−0.799625	−0.235320	−0.525864	0.074*
C10	−0.6730 (4)	−0.0165 (3)	−0.4264 (2)	0.0681 (7)
H10	−0.730846	0.012005	−0.498326	0.082*
C11	−0.5455 (4)	0.0906 (3)	−0.3042 (2)	0.0534 (6)
H11	−0.517565	0.190539	−0.294152	0.064*
C12	−0.2584 (4)	0.6538 (3)	0.0049 (3)	0.0625 (7)

H12A	−0.215116	0.743512	−0.011824	0.094*
H12B	−0.294736	0.676184	0.082561	0.094*
H12C	−0.372897	0.585240	−0.071673	0.094*

Atomic displacement parameters (Å²)

	U^{11}	U^{22}	U^{33}	U^{12}	U^{13}	U^{23}
V1	0.0405 (2)	0.03042 (18)	0.0430 (2)	0.00729 (14)	0.01466 (15)	0.01163 (14)
O1	0.0502 (9)	0.0411 (8)	0.0513 (9)	−0.0025 (7)	0.0044 (7)	0.0144 (7)
O2	0.0355 (7)	0.0337 (7)	0.0459 (8)	0.0062 (6)	0.0091 (6)	0.0146 (6)
O3	0.0379 (7)	0.0321 (7)	0.0557 (8)	0.0134 (6)	0.0187 (6)	0.0166 (6)
O4	0.0737 (11)	0.0503 (9)	0.0594 (10)	0.0227 (8)	0.0364 (9)	0.0188 (8)
N1	0.0509 (11)	0.0482 (11)	0.0458 (10)	0.0052 (9)	0.0016 (8)	0.0096 (8)
N2	0.0333 (8)	0.0333 (8)	0.0376 (8)	0.0067 (6)	0.0127 (7)	0.0102 (7)
N3	0.0358 (8)	0.0347 (8)	0.0356 (8)	0.0075 (7)	0.0113 (7)	0.0101 (7)
C1	0.0609 (15)	0.0654 (15)	0.0410 (12)	0.0124 (12)	0.0056 (11)	0.0138 (11)
C2	0.0405 (11)	0.0473 (12)	0.0406 (11)	0.0116 (9)	0.0098 (9)	0.0106 (9)
C3	0.0345 (10)	0.0413 (10)	0.0383 (10)	0.0114 (8)	0.0146 (8)	0.0130 (8)
C4	0.0535 (13)	0.0465 (12)	0.0470 (12)	0.0206 (10)	0.0148 (10)	0.0191 (10)
C5	0.0316 (9)	0.0366 (10)	0.0396 (10)	0.0067 (8)	0.0177 (8)	0.0131 (8)
C6	0.0316 (9)	0.0378 (10)	0.0391 (10)	0.0058 (8)	0.0153 (8)	0.0113 (8)
C7	0.0422 (11)	0.0410 (11)	0.0504 (12)	0.0095 (9)	0.0157 (9)	0.0146 (9)
C8	0.0523 (13)	0.0381 (11)	0.0623 (14)	0.0043 (10)	0.0213 (11)	0.0053 (10)
C9	0.0574 (14)	0.0589 (15)	0.0445 (13)	0.0026 (12)	0.0132 (11)	−0.0016 (11)
C10	0.0775 (18)	0.0694 (17)	0.0404 (12)	0.0095 (14)	0.0067 (12)	0.0199 (12)
C11	0.0619 (14)	0.0455 (12)	0.0437 (12)	0.0054 (10)	0.012 (1)	0.0183 (10)
C12	0.0553 (14)	0.0576 (14)	0.098 (2)	0.0325 (12)	0.0389 (14)	0.0391 (14)

Geometric parameters (Å, º)

V1—O4	1.5795 (16)	C4—H4A	0.9600
V1—O1	1.8200 (16)	C4—H4B	0.9600
V1—O3	1.8351 (14)	C4—H4C	0.9600
V1—O2	1.9469 (14)	C5—C6	1.475 (3)
V1—N2	2.1013 (16)	C6—C11	1.378 (3)
V1—O3[i]	2.3240 (14)	C6—C7	1.392 (3)
O1—N1	1.361 (2)	C7—C8	1.377 (3)
O2—C5	1.298 (2)	C7—H7	0.9300
O3—C12	1.433 (3)	C8—C9	1.369 (4)
N1—C2	1.289 (3)	C8—H8	0.9300
N2—C3	1.293 (2)	C9—C10	1.369 (4)
N2—N3	1.385 (2)	C9—H9	0.9300
N3—C5	1.308 (2)	C10—C11	1.382 (3)
C1—C2	1.499 (3)	C10—H10	0.9300
C1—H1A	0.9600	C11—H11	0.9300
C1—H1B	0.9600	C12—H12A	0.9600
C1—H1C	0.9600	C12—H12B	0.9600
C2—C3	1.472 (3)	C12—H12C	0.9600

C3—C4	1.491 (3)		
O4—V1—O1	100.13 (9)	N2—C3—C4	121.05 (18)
O4—V1—O3	103.30 (7)	C2—C3—C4	119.71 (18)
O1—V1—O3	107.22 (7)	C3—C4—H4A	109.5
O4—V1—O2	100.48 (8)	C3—C4—H4B	109.5
O1—V1—O2	149.15 (7)	H4A—C4—H4B	109.5
O3—V1—O2	90.01 (6)	C3—C4—H4C	109.5
O4—V1—N2	95.24 (7)	H4A—C4—H4C	109.5
O1—V1—N2	80.87 (6)	H4B—C4—H4C	109.5
O3—V1—N2	157.85 (6)	O2—C5—N3	123.23 (17)
O2—V1—N2	74.61 (6)	O2—C5—C6	118.16 (17)
O4—V1—O3ⁱ	177.40 (7)	N3—C5—C6	118.58 (17)
O1—V1—O3ⁱ	79.72 (7)	C11—C6—C7	119.27 (19)
O3—V1—O3ⁱ	74.33 (6)	C11—C6—C5	119.82 (18)
O2—V1—O3ⁱ	80.69 (6)	C7—C6—C5	120.85 (18)
N2—V1—O3ⁱ	87.30 (5)	C8—C7—C6	120.0 (2)
N1—O1—V1	129.68 (13)	C8—C7—H7	120.0
C5—O2—V1	117.55 (12)	C6—C7—H7	120.0
C12—O3—V1	124.15 (13)	C9—C8—C7	120.4 (2)
C12—O3—V1ⁱ	124.22 (14)	C9—C8—H8	119.8
V1—O3—V1ⁱ	105.67 (6)	C7—C8—H8	119.8
C2—N1—O1	116.97 (17)	C10—C9—C8	119.7 (2)
C3—N2—N3	117.28 (16)	C10—C9—H9	120.2
C3—N2—V1	126.48 (13)	C8—C9—H9	120.2
N3—N2—V1	116.22 (11)	C9—C10—C11	120.8 (2)
C5—N3—N2	107.95 (15)	C9—C10—H10	119.6
C2—C1—H1A	109.5	C11—C10—H10	119.6
C2—C1—H1B	109.5	C6—C11—C10	119.8 (2)
H1A—C1—H1B	109.5	C6—C11—H11	120.1
C2—C1—H1C	109.5	C10—C11—H11	120.1
H1A—C1—H1C	109.5	O3—C12—H12A	109.5
H1B—C1—H1C	109.5	O3—C12—H12B	109.5
N1—C2—C3	125.5 (2)	H12A—C12—H12B	109.5
N1—C2—C1	114.69 (19)	O3—C12—H12C	109.5
C3—C2—C1	119.7 (2)	H12A—C12—H12C	109.5
N2—C3—C2	119.24 (18)	H12B—C12—H12C	109.5
O4—V1—O1—N1	41.62 (19)	N3—N2—C3—C4	0.1 (3)
O3—V1—O1—N1	149.08 (17)	V1—N2—C3—C4	178.75 (14)
O2—V1—O1—N1	−89.6 (2)	N1—C2—C3—N2	−20.0 (3)
N2—V1—O1—N1	−52.12 (18)	C1—C2—C3—N2	163.8 (2)
O3ⁱ—V1—O1—N1	−141.01 (18)	N1—C2—C3—C4	160.6 (2)
O4—V1—O3—C12	−27.48 (19)	C1—C2—C3—C4	−15.7 (3)
O1—V1—O3—C12	−132.69 (18)	V1—O2—C5—N3	3.6 (2)
O2—V1—O3—C12	73.30 (18)	V1—O2—C5—C6	−174.43 (12)
N2—V1—O3—C12	118.6 (2)	N2—N3—C5—O2	1.7 (2)
O3ⁱ—V1—O3—C12	153.6 (2)	N2—N3—C5—C6	179.71 (15)

O4—V1—O3—V1ⁱ	178.90 (8)	O2—C5—C6—C11	13.4 (3)
O1—V1—O3—V1ⁱ	73.68 (8)	N3—C5—C6—C11	−164.71 (19)
O2—V1—O3—V1ⁱ	−80.33 (7)	O2—C5—C6—C7	−169.48 (17)
N2—V1—O3—V1ⁱ	−35.03 (18)	N3—C5—C6—C7	12.4 (3)
O3ⁱ—V1—O3—V1ⁱ	−0.001 (1)	C11—C6—C7—C8	1.9 (3)
V1—O1—N1—C2	48.4 (3)	C5—C6—C7—C8	−175.28 (19)
C3—N2—N3—C5	172.97 (16)	C6—C7—C8—C9	−0.9 (3)
V1—N2—N3—C5	−5.80 (18)	C7—C8—C9—C10	−0.6 (4)
O1—N1—C2—C3	0.3 (3)	C8—C9—C10—C11	1.1 (4)
O1—N1—C2—C1	176.7 (2)	C7—C6—C11—C10	−1.4 (3)
N3—N2—C3—C2	−179.30 (16)	C5—C6—C11—C10	175.8 (2)
V1—N2—C3—C2	−0.7 (3)	C9—C10—C11—C6	−0.1 (4)

Symmetry code: (i) −*x*, −*y*+1, −*z*.

Hydrogen-bond geometry (Å, º)

D—H···*A*	*D*—H	H···*A*	*D*···*A*	*D*—H···*A*
C1—H1*A*···O4ⁱⁱ	0.96	2.98	3.583 (3)	122
C1—H1*A*···N1ⁱⁱⁱ	0.96	3.02	3.508 (3)	113
C4—H4*A*···N3ⁱᵛ	0.96	2.81	3.663 (3)	149
C12—H12*B*···O2ᵛ	0.96	2.96	3.531 (3)	119
C12—H12*C*···O4ᵛ	0.96	2.81	3.629 (3)	144

Symmetry codes: (ii) −*x*, −*y*+1, −*z*+1; (iii) −*x*+1, −*y*+1, −*z*+1; (iv) −*x*, −*y*, −*z*; (v) −*x*−1, −*y*+1, −*z*.